

Superconductivity in mesoscopic high- T_c superconducting particles

V. A. Ivanov*, V. R. Misko**, V. M. Fomin^b, J. T. Devreese[#]
Theoretische Fysica van de Vaste Stoffen, Universiteit Antwerpen (U.I.A.),
Universiteitsplein 1, B-2610 Antwerpen, België
 (February 1, 2008)

Based on the Hubbard model in the framework of non-phonon kinematical mechanism and taking into account the discreteness of an electronic energy spectrum, the superconducting critical temperature of a mesoscopic high- T_c sphere is analyzed as a function of doping and as a function of a particle's radius. The critical temperature T_c is found to be an oscillating function of the radius of a particle. The size-dependent doping regime is revealed in high- T_c nanoparticles. Our analysis shows that each oscillation in T_c corresponds to the increase of a number of the energy levels in the sphere by one. The amplitude of oscillations of T_c increases with decreasing R and can reach a value of 6 K for nanopartilces with sizes about 25 nm, in a good agreement with experimental studies of $\text{YBa}_2\text{Cu}_3\text{O}_{7-\delta}$ nanoparticles.

PACS numbers: 74.72.Bk; 74.62.Dh; 74.20.-z

I. INTRODUCTION

After experiments by Ralph *et al.*^{1,2} on the electronic states in nanosize *Al* particles there has been increasing experimental and theoretical interest in properties of ultrasmall superconducting samples with discrete fermionic energy spectrum (see^{3,4} and Refs therein). Incorporation of the nanosize particles as a part of single-electron tunneling transistor schemes allowed for measurements of excitation spectra as a function of the number of electrons in a superconducting particle. The large spectroscopic gap between the lowest energy level and all the others which can be driven to zero by application of magnetic fields has been explained by superconducting pairing.

Till now experiments have been completed for the low T_c elemental superconductors (Al, Sn, ...), showing traces of superconducting pairing for metallic particles even with the electron energy spacing being larger than the superconducting energy gap: $d > \Delta$. For elemental superconductors in the order of magnitude $\Delta \sim T_c$, the energy spacing is $d \sim \hbar^2/(m_e R^2)$ and for these nanoparticles their size $R \lesssim \hbar/\sqrt{m_e T_c}$. Thus, to satisfy the regime $d \gtrsim \Delta$ for characteristic critical temperature values $T_c \sim 1\text{K}$ the nanoparticle size should not exceed $\sim 30\text{ nm}$ ⁵. As shown by Tinkham team, the problems of the sample preparation with these parameters have been solved by modern technology. In such nanoparticles from elemental superconductors their average size is smaller or comparable with the coherence length and fluctuations of superconducting order parameter do not allow the mean-field treatment. On this way the recent theoretical work includes studies of mesoscopic systems with equally spaced levels⁶, Wigner-Dyson level spacing⁷, parity effect⁸, fluctuation effects⁹, fixed-N canonical treatment¹⁰ and the suppressing role of the non-pair portion of the interaction¹¹. The differences in energy level spectra for even and odd numbers of electrons are being interpreted as a result of superconducting paring interactions.

But today the nanotechnology is on the threshold of production of nanosize samples from high- T_c cuprates¹²⁻¹⁴. More recently, a several degrees enhancement of the onset transition temperature T_c has been observed in superconducting dots formed by the high- T_c superconductor $\text{YBa}_2\text{Cu}_3\text{O}_{7-\delta}$ (YBCO)¹⁵ and in $\text{YBa}_2\text{Cu}_3\text{O}_{7-\delta}$ films with detected spherical particles on their surface¹³. The dots were formed when powder YBCO particles with a diameter $\leq 600\text{ nm}$ were exposed to a RF plasma to produce a Coulomb crystal. The plasma damaged the particles and caused 20-25 nm sized isolated islands of the correct stoichiometry to segregate within each particle. Possible technological applications of superconducting nanoparticles make it desirable, to engineer their energy spectra and the pairing characteristics. The crucial question that has arisen in this connection is: how can the superconducting critical temperature for a high- T_c nanoparticle be controlled by changing its size and the doping degree?

In nanoparticles made from high- T_c materials it's questionable to reach the regime $d > \Delta$ corresponding to size $R \lesssim \hbar/\sqrt{m\Delta} = \hbar\sqrt{2}/\sqrt{mT_c(2\Delta/T_c)}$. Really for high- T_c superconductors the BCS ratios $2\Delta/T_c$ are quite large (9 for $\text{La}_{2-x}\text{Sr}_x\text{CuO}_4$, 6-8 for $\text{YBa}_2\text{Cu}_3\text{O}_{7-\delta}$, and even 12 for $\text{Bi}_2\text{Sr}_{2-x}\text{La}_x\text{CuO}_6$ - see¹⁶ and Refs. therein) and the magnitudes of an effective electron mass m are enhanced due to narrow energy bands of high- T_c materials. As a result, the high- T_c nanoparticle size R is becoming comparable with a unit cell size (it's lattice constant parameter $c \simeq 1.2\text{ nm}$ in YBCO) or even less than the latter with a significant deviations of a chemical composition and the intra-size vibrations from those in a bulk mother substance. Physically, it means that for the nanosize particles formed from stoichiometric high- T_c material we can not reach regime $\Delta < d$. Thus, the field of the nano-size high- T_c superconductors is renewing the earlier Anderson idea¹⁷ about the disappearance of superconductivity in particles,

which are so small that the “granularity” of an electron energy d is larger than the superconducting energy gap Δ . So, for the nanosized high- T_c particles we are returning back to the limit $d < \Delta$.

Long time ago the studies of the superconducting-transition temperature T_c of metallic films of Al, Sn, In, Zn prepared by vacuum deposition onto substrate held at cryogenic temperatures revealed the quantum size effect of the T_c -oscillations with a film thickness^{18–24} (see also review²⁵). In the simplest approaches^{26–28} the quantum size effects follow from oscillations in the electronic density of states with thickness which in turn lead to oscillations with thickness of T_c and other film quantities.

Here in the Anderson regime $d < \Delta$ we consider a similar mechanism of finite-size effects aiming the goal to apply it to realistic high- T_c nano-particles. Worthy to note, that an evaluated size of nanoparticles under consideration (see next section) exceeds the small coherence length scale with neglect of fluctuations and the Aslamazov-Larkin effect²⁹. The method is based on the study of the non-phonon kinematical superconductivity (see³⁰ and references therein) in systems with strongly interacting electrons and an intrinsic “granularity” of energy, induced by the discreteness of electron energy levels in a nanoparticle. Formally the non-phonon mechanism allows to avoid difficulties caused by phonon cut-off energies in small particles. In the model we assume the boundary condition on the electronic wave-functions is that they vanish on the surface of spherical nanoparticle and we neglect the surface effects.

II. THE MODEL

In the present communication we tackle the problem starting from the strongly interacting limit of the Hubbard model ($U \gg t$), $H = -\sum t_{ij} X_i^{\sigma 0} X_j^{0\sigma} - \mu \sum n_i$, for correlated electrons (μ : their chemical potential, n_i : electron density operator on site, t_{ij} : intersite electron hopping) in the YBCO nanoparticles of a spherical shape. As usual, $X^{0\sigma}$ denote a projection Hubbard operator with an index “ 0σ ” labeling an intrasite transition from an energy level occupied by an electron with spin projection σ to an empty one: $\sigma \rightarrow 0$. In high- T_c materials the characteristic strong electron interactions remove the orbital degeneracy of energy levels. The electron energies have been extracted^{30,31} from zeros of the inverse Green’s function, obeying the Dyson equation

$$\mathcal{D}^{-1}(i\omega) = [\mathcal{D}^0(i\omega)]^{-1} + t_{ij}, \quad (1)$$

where the first order self-energy is itself an electron hopping t_{ij} inside a spherical nanoparticle. The zeroth order Green’s function is defined as $\mathcal{D}^0(\tau) = -\langle \hat{T} X^{0\sigma}(\tau) X^{\sigma 0}(0) \rangle$ or in Matsubara $\omega = (2n+1)\pi T$ -representation it is such as

$$\mathcal{D}^0(i\omega) = \frac{f}{-i\omega_n - \mu}. \quad (2)$$

The correlation factor,

$$\begin{aligned} f &= \langle X^{00} + X^{\sigma\sigma} \rangle = 1 - \langle X^{\bar{\sigma}\bar{\sigma}} \rangle \\ &\equiv 1 - n_{\bar{\sigma}} = 1 - \frac{n}{2} = \frac{1+x}{2}, \end{aligned} \quad (3)$$

is governed by an average electron density per site n or/and by a doping parameter $x = 1 - n$ ($0 \leq x \leq 1$).

In the momentum representation of bulk material the correlated electron energy is $\xi = ft_p - \mu$ with an energy dispersion values t_p located inside the band: $-w \leq t_p \leq w$. The superconducting instability is driven by the homogeneous Bethe-Salpeter equation for a vertex Γ of two scattering fermions with opposite spin orientations and opposite momenta in their reference system:

$$\Gamma = 2T \sum_{p,n} t_p G_{-\omega}(-p) G_{\omega}(p) \Gamma(p), \quad (4)$$

where $G_{\omega}(p) = (-i\omega + \xi_p)^{-1}$ is the normal Green’s function. After summation over Matsubara frequencies this equation can be converted to equation

$$1 = \sum_p \frac{t_p}{ft_p - \mu} \text{th} \frac{ft_p - \mu}{2T_c}, \quad (5)$$

represented in momentum representation.

In the experiment¹⁵ both the initial YBCO material and nanosized (20-25 nm) islands produced by plasma damage are polycrystalline particles with chaotic distribution of crystallographic directions. Therefore, we can model each nanosized island by isotropic sphere of radius R . As in the case of dirty superconductors¹⁷, in a spherical particle of radius R with the quantized electronic energy levels, $E_\nu = \hbar^2 \nu^2 / (2mR^2)$, the momenta are not good quantum numbers. In the absence of non-elastic processes the suitable quantum numbers are the eigen-energies of the problem, shifted by a half-bandwidth w : $\epsilon_\nu = E_\nu - w$ ($-w \leq \epsilon_\nu \leq w$). For HTSC's of interest such as $\text{YBa}_2\text{Cu}_3\text{O}_{7-\delta}$ a half-bandwidth parameter has characteristic magnitude $w \sim 0.5$ eV³². The lowest energy level is at the bottom of the starting bulk energy band, $\epsilon_0 = -w$, whereas the highest one, ϵ_{ν_0} , coincides with the top of the band: $\nu_0 = [R\sqrt{2mw}/\hbar]$ ([...] stands for an integer number). So, in an energy representation the superconducting critical temperature T_c is determined by the following equation:

$$1 = \frac{1}{\nu_0} \sum_{\nu=1}^{\nu_0} \frac{\frac{E_\nu}{w} - 1}{\left(\frac{E_\nu}{w} - 1\right)f - \frac{\mu}{w}} \tanh\left(\frac{\left(\frac{E_\nu}{w} - 1\right)f - \frac{\mu}{w}}{\frac{2T_c}{w}}\right), \quad (6)$$

where the summation is running over quantized energy levels till the upper level ν_0 ; the chemical potential μ has a meaning of the highest occupied energy level. The doping parameter x is defined by

$$1 - x = 2T \sum_{n, \nu=1}^{\nu_0} e^{i\omega_n \delta} \mathcal{D}(\nu, \omega_n). \quad (7)$$

From here one can find the equation for the chemical potential μ :

$$\frac{1-x}{1+x} = \frac{R}{\hbar\nu_0} \sqrt{\frac{m}{2} \left(\frac{2\mu}{1+x} + w \right)}. \quad (8)$$

The system of equations, Eqs. (6), (8) should be solved self-consistently to obtain T_c .

The applied arithmetics is valid until the superconducting pairing is allowed for electrons belonging to different energy levels in a nanoparticle, *i.e.* the thermal energy should exceed the distance between the discrete energy levels, namely $T_c > \hbar^2 [\nu_0^2 - (\nu_0 - 1)^2] / (2mR^2)$, wherefrom it follows the restriction for the high- T_c nanoparticle radii in our approach:

$$R > R_0 = \frac{2\hbar}{T_c} \sqrt{\frac{w}{m}}.$$

For estimate we assume the effective mass enhancement $m/m_e \approx 10$ from the earlier optical reflectivity measurements³³ for the YBCO bulk crystals. Noteworthy, the more recent data for YBCO³⁴ give closed estimate $m \approx 8 - 9m_e$ under the assumption of a twice band mass enhancement due to electron correlations: $m_b = 2m_e$. Such estimate $m \approx 10m_e$ is also in an agreement with theoretical evaluations^{35,36} for an effective electron mass in YBCO. Finally, for the YBCO nanoparticle of interest¹⁵ with $T_c = 92$ K and a half-bandwidth $w = 0.725$ eV (this value of w corresponds in our calculations to the "bulk" critical temperature $T_c = 92$ K) one can conclude *the lower critical radius of a spherical YBCO nanoparticle such as $R_0 = 15$ nm to apply the theory.* The nanoparticle with a critical radius still contains $75\pi \cdot 10^3$ unit cells of YBCO (the YBCO unit cell volume is ~ 0.18 nm³), which is in a reasonable agreement with a neglect of surface and fluctuation effects. As it will be seen from numerical results in next sections, although we are working in the bulk superconducting regime, the quantum size effects due to a "granularity" of an energy in high- T_c nanosize particles are still traced.

III. RESULTS AND DISCUSSION

A. The critical temperature T_c of a mesoscopic high- T_c superconducting sphere as a function of doping x

Based on Eqs. (6) and (8), we analyze the critical temperature of a mesoscopic high- T_c superconducting sphere as a function of doping. We have performed calculations for various radii R of a superconducting sphere varying from $R = 15$ nm to 1000 nm. In Fig. 1, the critical temperature T_c of a mesoscopic high- T_c superconducting sphere is plotted as a function of doping x for particles with radii $R = 15$ nm, 16 nm, 20 nm, 30 nm and 1000 nm. For any radius within the above region, T_c as a function of x is characterized by the following behavior: T_c is zero until some

minimal doping x_{min} , which provides a particle to be superconducting; then T_c increases (underdoped regime) and reaches a maximum at some value of doping (optimal doping); further increase of x leads to decrease of T_c (overdoped regime) (see Fig. 1).

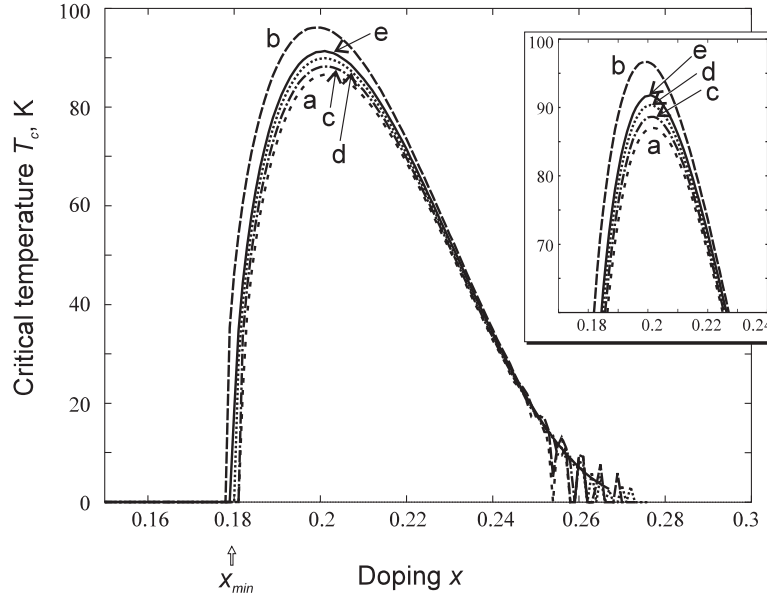


FIG. 1. The critical temperature T_c as a function of doping x , for a mesoscopic high- T_c superconducting spherical particle. The radii of the particles are $R = 15$ nm (a), 16 nm (b), 20 nm (c), 30 nm (d) and 1000 nm (e). The value of the bandwidth parameter for $\text{YBa}_2\text{Cu}_3\text{O}_{7-\delta}$ is $w = 0.725$ eV. The inset shows upper parts of the curves $T_c = T_c(x)$ for temperatures ranging in the interval from 60 to 100 K.

The maximal value of $T_c = T_c(x)$ is a non-monotonous function of R . For example, at $R = 15$ nm the maximum of T_c is 86.6 K, whereas at $R = 16$ nm the maximum value of T_c is as high as 96.1 K. With increasing radius, a deviation in the maximal value of T_c reduces, and for large radii (more than 100 nm) the maximal values of T_c are close to each other and lie in the vicinity to $T_c \approx 92$ K. A further increase of the radius of the sphere does not lead to any appreciable changes of T_c .

A position of the maximum of $T_c = T_c(x)$ itself also varies as a function of radius R . For $R = 15$ nm, the maximum of $T_c = T_c(x)$ is reached at a higher x as compared to “bulk” value ($R = 1000$ nm). On the contrary, for $R = 16$ nm, the maximum of $T_c = T_c(x)$ is at a lower x as compared to the “bulk” value.

The critical temperature of a mesoscopic high- T_c superconducting sphere as a function of doping is characterized by some minimal value of doping and by oscillating behaviour in strongly overdoped regime (see Fig. 1). Although the critical temperature of a mesoscopic high- T_c superconducting sphere is itself a smooth function of doping, the minimal doping x_{min} occurs to be an oscillating function of the radius of the particle. The minimal doping, which provides the particle to be superconducting, is very sensitive to the bandwidth parameter w . Varying the parameter w , we can conclude that reduction of the bandwidth leads to increase of the average value of x_{min} and to decrease of the period of oscillations.

B. The critical temperature of a mesoscopic high- T_c superconducting sphere versus its radius

In this section, we analyze in detail the oscillations in T_c that were noted in the previous subsection. The critical temperature T_c is calculated as a function of the radius R of the sphere for various values of doping x . In Fig. 2, $T_c = T_c(R)$ is shown for $x = 0.2$ (that is close to the optimal doping). The critical temperature T_c as a function of radius R is characterized by an oscillating behavior. The amplitude of these oscillations decreases with increasing R . It is maximal at small R : $T_c = T_c(R)$ varies from about 86.4 K up to 97.8 K in the interval from $R = 15$ nm to 18 nm (see the upper inset to Fig. 2). Then, as shown in the bottom inset to Fig. 2, the amplitude of the oscillations decreases very fast up to $R \approx 100$ nm. For larger R , $T_c = T_c(R)$ is characterized by a slow decrease versus R . The function $T_c = T_c(R)$ “saturates” with increasing R and reaches the “bulk” value 92 K.

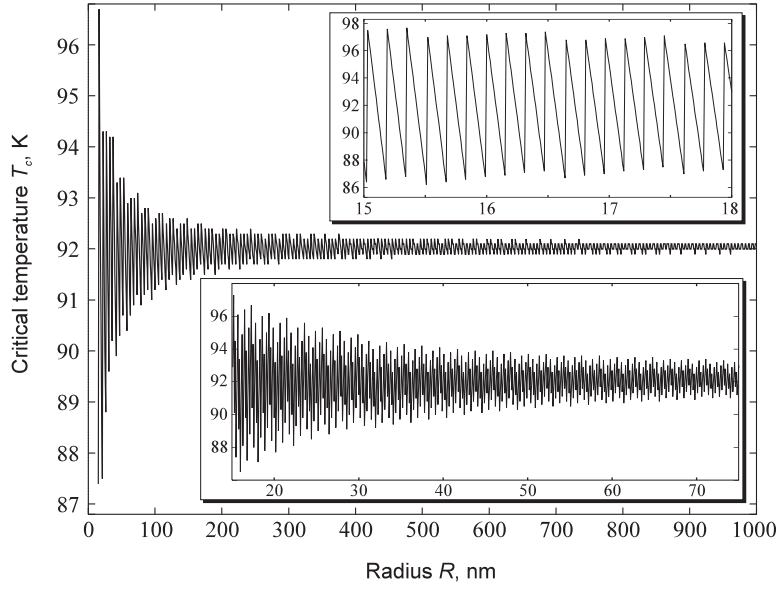


FIG. 2. The critical temperature T_c as a function of the radius R of a mesoscopic high- T_c superconducting particle, at the optimal doping $x = 0.2$, for radii from $R = 15$ nm to 1000 nm. In the bottom inset: T_c as a function R for radii from $R = 15$ nm to 75 nm. The top inset: $T_c = T_c(R)$ for $R = 15$ nm to 18 nm. Each oscillation in $T_c = T_c(R)$ corresponds to the change of the number of levels in the system by one.

The oscillations in the function $T_c = T_c(R)$ are due to the discrete density of states in the superconducting sphere. Recall that we analyze high- T_c spheres with a confinement of carriers in all three dimensions. Our analysis shows that each oscillation in T_c with increasing R corresponds to the increase of a number of the energy levels in the sphere by one.

In the overdoped regime, the function $T_c = T_c(R)$ is analyzed for $x = 0.225$. The results of the calculations are shown in Fig. 3 for $R = 15$ nm to 1000 nm. The “bulk” value of T_c for $x = 0.225$ ($T_{c,bulk} = 62.4$ K) is much lower than that for the optimal doping. Therefore, slowly varying the doping parameter x , we can model various real samples used in experiments.

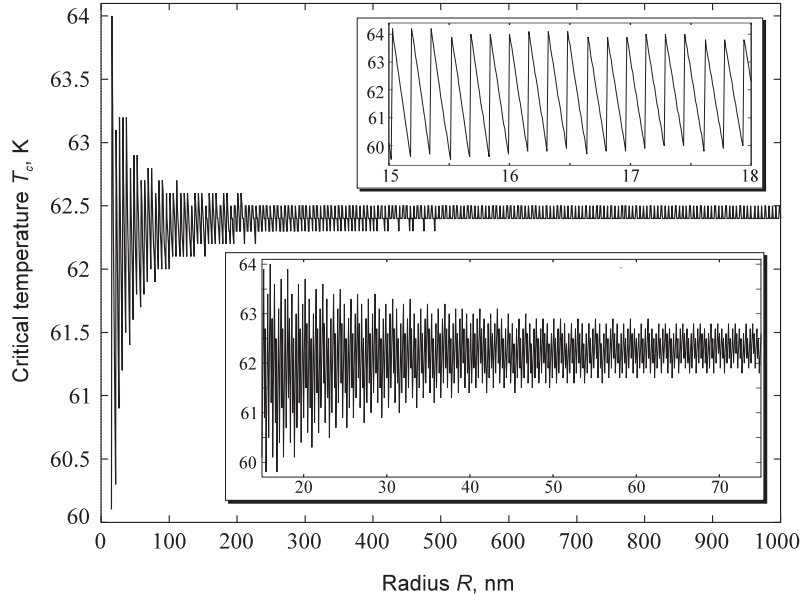


FIG. 3. The critical temperature T_c as a function of R in the overdoped regime, $x = 0.225$. The range of particles radii and the bandwidth parameter are the same as in Fig. 2.

In the paper by Menon *et al.*¹⁵, a slight enhancement in the critical temperature T_c was detected for $\text{YBa}_2\text{Cu}_3\text{O}_{7-\delta}$ plasma-damaged nanoparticles with sizes about 25 nm. To find the transition temperature in the particles, their dc

susceptibility was measured as a function of temperature in a SQUID magnetometer. The transition temperature for the onset of superconductivity is defined as the temperature at which the susceptibility begins to drop¹⁵. In some cases, the increase in critical temperature was only 1 K ($T_{c,bulk} = 92$ K), whereas the increase reached 6 K for some other samples¹⁵. From our calculations it follows that, for the optimal doping (characterized by the “bulk” value $T_{c,bulk} = 92$ K) the enhancement of the critical temperature for nanoparticles with the radii $R = 15$ nm to $R = 18$ nm can be up to 6 K (see upper inset to Fig. 2). This is in a rather good agreement with the experimental results¹⁵. Moreover, the revealed oscillations of T_c as a function of R explain the non-regular character of the enhancement of T_c in different samples¹⁵.

IV. CONCLUSIONS

The superconducting critical temperature of a mesoscopic high- T_c sphere has been analyzed as a function of doping and as a function of a particle’s radius. The approach is based on the Hubbard model as the most fundamental model of the electronic interactions in high- T_c materials. Quantum Monte Carlo studies of this model (see³⁷ and references therein) concluded that the enhanced superconducting correlations are not predominant at low temperatures or in the ground state. Although some of numerical works supported the existence of superconducting pairing in the Hubbard model^{38,39}, these quantum Monte Carlo computations have restricted parameter space such as the system size, the doping, the low values of the Hubbard energy etc. The modern Monte Carlo^{40–42} and other⁴³ methods allow one to treat a wider parameter space with large magnitude of the Hubbard energy and reveal the superconducting correlations in the ground state of the two-dimensional Hubbard model. So, the numerical simulation of superconductivity in the ground state of the Hubbard model still remains the issue for the serious problem of the two-dimensional nature of cuprate high- T_c superconductors. As distinct from that, the kinematical mechanism (see Ref.³⁰ and references therein) considers the superconducting instability of strongly correlated electrons in normal state beyond the knowledge of their ground state properties. Therefore the present study of superconductivity is based on the non-phonon kinematical mechanism in the framework of the Hubbard model taking into account the “granularity” of electron energies (the discreteness of an electronic energy spectrum) in nanoparticles. The chaotic crystallite structure allowed us to model nanoparticles by the isotropic spherical particles. This point made suitable the applied three-dimensional scenario of the kinematical attraction for YBCO nanoparticles under study. Worthly to note that in one-band two-dimensional Hubbard model the kinematical superconducting instability occurs at bulk doping $x < 1/3$ as in variational Monte Carlo method (see, e.g., Ref.⁴⁰). Stimulated by the recent successful results on technology of a nano-sample preparation from YBCO^{12–15}, the typical superconducting compound $\text{YBa}_2\text{Cu}_3\text{O}_{7-\delta}$ has been taken as a mother substance forming the nanoparticle. We have shown that the critical temperature of a mesoscopic high- T_c superconducting sphere is characterized by a non-monotonic dependence on doping as in bulk material. However, contrary to the bulk high- T_c materials the T_c -maximum (corresponding to the optimal doping) is shifted to the lower doping regime. A bulk material with a decreased T_c value in overdoped regime can form a nanoparticle with a maximal T_c value which means that it is in an effective optimally doped regime. Also an optimally doped bulk high- T_c material behaves as an underdoped substance in nanoparticles. The revealed size-dependent doping regime in high- T_c nanoparticles is new effect in comparison with quantum size effects in elemental low- T_c nanoparticles.

Although we worked in the Anderson regime $d < \Delta$, *i.e.* neglecting the parity effects, and due to the small coherence length of high- T'_c s, $\xi < R_0 = 15$ nm, neglecting the fluctuation effects, it have been established that the critical temperature of a mesoscopic high- T_c superconducting sphere is an oscillating function of a large sphere size $R > R_0$. For sphere radii with value $R \gtrsim 1000$ nm and doping $x = 0.2 - 0.25$ the T_c -oscillations actually disappear. The oscillating quantum size effects appear whenever a size-dependent energy level passes through the chemical potential as the size of a nanosphere is varied. At each resonance a new quantized energy level starts to contribute to an electron density of states and superconducting quantities. For chemical potential nearly zero ($x \sim 1/3$) this oscillating behaviour is more pronounced and results in new T_c oscillations with doping in strongly overdoped regime (cf. Fig. 1). The amplitude of T_c -oscillations is enhanced for lower radii of mesoscopic spheres. For an electron confined to a sphere of radius R , the radial part of the wave function is proportional to $j_1(kR)$, *i.e.* to $\sin(kR)/kR$ for electrons without angular momenta. Therefore the boundary condition yields the relationship $kR = n\pi$ with a period of oscillations such as $\Delta R = \pi/k = \lambda_F/2$, a half of de Broglie wave-length. The calculations are performed for spherical YBCO nanoparticles which radius exceeds the critical one $R_0 = 15$ nm. The nanoparticle with a critical radius R_0 still contains $75\pi \cdot 10^3$ unit cells of YBCO (the YBCO unit cell volume is ~ 0.180 nm³). For the optimally doped regime, the enhancement of the superconducting critical temperature for the particles with sizes $R = 25$ nm can be up to 6 K what is in agreement with the experimental findings for $\text{YBa}_2\text{Cu}_3\text{O}_{7-\delta}$ nanoparticles in Ref.¹⁵. Also we can not exclude the visualized enhancement $\Delta T_c \gtrsim 1\text{K}$ in $\text{YBa}_2\text{Cu}_3\text{O}_{7-\delta}$ films in Ref.¹³ due to detected spherical particle formation on their surface in the process of laser ablation with increased deposition temperatures

$> 790^0$ C. The developed theoretical approach can be applied to nanoparticles prepared from other high- T_c materials with narrow electronic energy bands in bulk.

Acknowledgements - We acknowledge useful discussions with F. Brosens. This work has been supported by GOA BOF UA 2000, IUAP, the FWO-V projects Nos. G.0306.00, G.0274.01, WOG WO.025.99N (Belgium), and the ESF Programme VORTEX.

-
- * On leave from N. S. Kurnakov Institute of General and Inorganic Chemistry of the Russian Academy of Sciences, Leninskii prospekt 31, 117907 Moscow, Russia
- ** On leave from Department of Theory of Semiconductors and Quantum Electronics, Institute of Applied Physics, Academy of Sciences of Moldova, Str. Academiei 5, MD-2028 Kishinev, Republic of Moldova
- ^b On leave from Department of Theoretical Physics, State University of Moldova, Str. A. Mateevici 60, MD-2009 Kishinev, Republic of Moldova
- [#] Also at: Universiteit Antwerpen (RUCA), Groenenborgerlaan 171, B-2020 Antwerpen, België and Technische Universiteit Eindhoven, P. O. Box 513, 5600 MB Eindhoven, The Netherlands
- ¹ D. C. Ralph, C. T. Black, and M. Tinkham, Phys. Rev. Lett. **74**, 3241 (1995).
- ² D. C. Ralph, C. T. Black, and M. Tinkham, Phys. Rev. Lett. **78**, 4087 (1997).
- ³ J. von Delft and D. C. Ralph, Physics Reports, **345**, 61 (2001).
- ⁴ J. von Delft, Ann. Phys. (Leipzig), **10**, 3, 1 (2001).
- ⁵ Y. Murayama, *Mesoscopic Systems (Fundamentals and Applications)* Wiley-VCH, Weinheim-N.Y.-Chichester-Brisbane-Singapore-Toronto, 2001).
- ⁶ J. von Delft, A. D. Zaikin, D. S. Golubev, W. Tichy, Phys. Rev. Lett. **77**, 3189 (1996).
- ⁷ R. A. Smith and V. Ambegaokar, Phys. Rev. Lett. **77**, 4962 (1996).
- ⁸ K. A. Matveev and A. I. Larkin, Phys. Rev. Lett. **78**, 3749 (1997).
- ⁹ R. A. Smith and V. Ambegaokar, Phys. Rev. Lett. **77**, 4962 (1996).
- ¹⁰ F. Broun, J. von Delft, D. C. Ralph, and M. Tinkham, Phys. Rev. Lett. **79**, 921 (1997).
- ¹¹ V. H. Crespi and M. L. Cohen, Phys. Rev. B **62**, 8669 (2000).
- ¹² D. B. Geohegan, A. A. Puretzky, and D. J. Rader, Appl. Phys. Lett. **74**, 3788 (1999).
- ¹³ P. B. Mozhaev, F. Rönning, P. V. Komissinskii, Z. G. Ivanov, and G. A. Ovsyannikov, Physica C **336**, 93 (2000).
- ¹⁴ Y. Zhao, S. H. Han, H. Zhang, and C. H. Choi, Physica C **337** 1-4, 106 (2000).
- ¹⁵ L. Menon, D. Yu, P. F. Williams, S. Bandyopadhyay, Y. Liu, and B. Jayaram, Solid State Commun. **117**, 615 (2001).
- ¹⁶ E. G. Maksimov, Physics-Uspexhi **170**, 1033 (2000).
- ¹⁷ P. W. Anderson, J. Phys. Chem. Solids **11**, 28 (1959).
- ¹⁸ N. V. Zavaritzky, Doklady Akademii nauk SSSR (Reports of the USSR Academy of Sciences - in Russian) **82**, 229 (1952); *ibid.* **86**, 501 (1952).
- ¹⁹ I. S. Khukhareva, Sov. Phys. JETP **16**, 828 (1963).
- ²⁰ M. Strongin, O. F. Kammerer, and A. Paskin, Phys. Rev. Lett. **14**, 949 (1965).
- ²¹ B. Abeles, R. W. Cohen, and G. W. Cullen, Phys. Rev. Lett. **17**, 632 (1966).
- ²² Yu. F. Komnik, E. I. Bukshtab, and K. K. Mankovskii, Sov. Phys. JETP **30**, 807 (1970).
- ²³ M. Strongin, O. F. Kammerer, J. E. Crow, B. D. Parks, D. H. Douglass, Jr., and M. A. Jensen, Phys. Rev. Lett. **21**, 1320 (1968).
- ²⁴ B. G. Orr, H. M. Jaeger, and A. M. Goldman, Phys. Rev. Lett. **53**, 2046 (1984).
- ²⁵ B. A. Tavger and V. Ya. Demikhovskii, Sov. Phys. Usp. **11**, 644 (1969).
- ²⁶ C. J. Thomson and J. M. Blatt, Phys. Lett. **5**, 6 (1963); J. M. Blatt and C. J. Thomson, Phys. Rev. Lett. **10**, 332 (1963).
- ²⁷ A. Paskin and A. D. Singh, Phys. Rev. **140**, A1965 (1965).
- ²⁸ D. A. Kirzhnits and E. G. Maksimov, JETP Lett. **2**, 274 (1966).
- ²⁹ L. G. Aslamazov and A. I. Larkin, Physics Letters **26A**, 238 (1968).
- ³⁰ V. A. Ivanov, Europhys. Lett. **52**, 351 (2000).
- ³¹ V. A. Ivanov, J. Phys.: Condens. Matter **6**, 2065 (1994); in *Studies of High- T_c Superconductors*, ed. by A. Narlikar (Nova Science, New York, 1993), Vol. 11, pp. 331-352; Physica C **271**, 127 (1996); Philos. Mag. B **76**, 697 (1997).
- ³² R. J. Radtke and M. R. Norman, Phys. Rev. B **50**, 9554 (1994).
- ³³ G. A. Thomas, J. Orenstein, D. H. Rapkine, M. Cappizzi, A. J. Millis, R. N. Bhatt, R. L. Schneemeyer, and J. V. Waszczak, Phys. Rev. Lett. **61**, 1313 (1988).
- ³⁴ D. N. Basov, C. C. Homes, E. J. Singley, M. Strongin, T. Timusk, G. Blumberg, and D. van der Marel, Phys. Rev. B **63**, 134514 (2001).

- ³⁵ A. La Magna, R. Pucci, Phys. Rev. B **55**, 14886 (1997).
- ³⁶ A. S. Alexandrov and V. V. Kabanov, Phys. Rev. B **59**, 13628 (1999).
- ³⁷ E. Dagotto, Rev. Mod. Phys. **66**, 763 (1994).
- ³⁸ J. E. Hirsch, Phys. Rev. Lett. **54**, 1317 (1985).
- ³⁹ T. Husslein, I. Morgenstern, D. M. Newns, P. C. Pattnaik, J. M. Singer, and H. G. Matutis, Phys. Rev. B **54**, 16179 (1996).
- ⁴⁰ T. Giamarchi and C. Lhuillier, Phys. Rev. B **43**, 12943 (1991).
- ⁴¹ T. Yanagisawa, S. Koike, and K. Yamaji, J. Phys. Soc. Jpn. **67**, 3867 (1998); Phys. Rev. B **64**, 184509 (2001).
- ⁴² K. Yamaji, M. Miyazaki, and T. Yanagisawa, Proceedings of LT-23, Hiroshima, 21-27 Aug. 2002.
- ⁴³ Th. Maier, M. Jarell, Th. Pruschke, and J. Keller, Phys. Rev. Lett. **85**, 1524 (2000).